Precision Engineering 76 (2022) 305–313

Contents lists available at ScienceDirect

Precision Engineering

journal homepage: www.elsevier.com/locate/precision

Plasma-induced atom migration manufacturing of fused silica

Rulin Li [a], Yaguo Li [b], Hui Deng [a,*]

[a] Department of Mechanical and Energy Engineering, Southern University of Science and Technology (SUSTech), No. 1088, Xueyuan Road, Shenzhen, Guangdong, 518055, China
[b] Fine Optical Engineering Research Centre, Chengdu, 610041, China

ARTICLE INFO

Keywords:
Atomic and close-to-atomic scale manufacturing
Atom migration
Polishing
Roughness

ABSTRACT

In this study, we report an ultra-precision nonsubtractive surface polishing technique named plasma-induced atom migration manufacturing (PAMM). In PAMM, the molten layer of the fused silica surface can be formed owing to the energy transmitted by inductively coupled plasma (ICP) which has a high gas temperature and radical density. The smoothing of surface is attributed to the rearrangement of surface atoms or clusters driven by surface tension. Unlike conventional subtractive smoothing processes, PAMM removes no material and can achieve damage-free surface with high efficiency and low cost, which makes it a promising technique to obtain large optical components with excellent optical performance and long operation life. The static and scanning smoothing characteristics of PAMM were presented and the surface smoothing mechanism was discussed. By this method, an ultrasmooth surface with Sa roughness of 0.15 nm was achieved. Furthermore, the validity of PAMM of spherical surface polishing and damaged surface recovering of fused silica was experimentally verified.

1. Introduction

Polishing is a widely used fine finishing process for high-value-added manufacturing such as that of semiconductor chips and optical components [1]. With the increasing requirements on surface parameters such as roughness, integrity and damage, the development of polishing processes is evolving from the conventional abrasion-based mechanical polishing (MP) to the newly advocated chemical-assisted hybrid polishing [2]. In MP processes, hard abrasives with sharp edges are used to deform the workpiece surface to realize material removal. However, surface damage, such as scratches and amorphous layers, and subsurface damage, such as cracks, stress and defects, are inevitably introduced [3]. To solve this problem, some chemical-assisted hybrid polishing techniques have been proposed in the past decades, among which chemical mechanical polishing (CMP) has become the most successful technology utilized by industry [4]. CMP is based on an efficient combination of the chemical modification of a hard surface and abrasion-based removal of the modified layer. With a precise control of the balance between chemical modification and mechanical removals, atomic scale polishing has been realized in various materials [5,6], including silicon wafers [7,8], fused glass [9,10], sapphire [11], silicon carbide (SiC) [12,13], and gallium nitride (GaN) [14]. In CMP process, the pH value of slurry and abrasives are important factors involved. To further improve the polishing efficiency and surface quality, various researches focused on slurry and abrasives have been developed, such as alkaline SiO_2 based slurry, acid SiO_2 based slurry [9], alkaline CeO_2 based slurry [15]as well as hydrogen peroxide added CeO_2 slurry [8].

In recent years, hybrid polishing processes also have been proposed such as photoelectrochemical mechanical polishing (PECMP) [16], catalyst-referred etching (CARE) [17], and plasma-assisted polishing (PAP) [18]. Although most of these techniques are still under development, achievements on ultrasmooth surfaces with atomic level roughness have been widely reported [19]. PECMP applied the ultraviolet-light irradiation to the GaN wafer surface to generate unpaired electron-holes during a mechanical polishing process. The free-holes facilitated photoelectrochemical oxidation so as to accelerate material removal in the polishing process. With the addicted ultraviolet-light irradiation, this method achieved a material removal rate of 1.2 μm/h which was one order of magnitude higher than that of a conventional CMP technique. And it removed the surface and subsurface damages induced in a previous machining process and obtained an atomically flat surface with Ra roughness of 0.067 nm in 1×1 μm^2. CARE utilized pure water and Pt as the etching solution and catalyst, while the apparatus for CARE was nearly the same as that of CMP, the technique mainly differed in the addition of a catalytic function on the pad surface by the deposition of a thin catalyst film. The etching solution

* Corresponding author.
E-mail address: dengh@sustech.edu.cn (H. Deng).

https://doi.org/10.1016/j.precisioneng.2022.04.005
Received 30 October 2021; Received in revised form 9 March 2022; Accepted 7 April 2022
Available online 12 April 2022
0141-6359/© 2022 Elsevier Inc. All rights reserved.

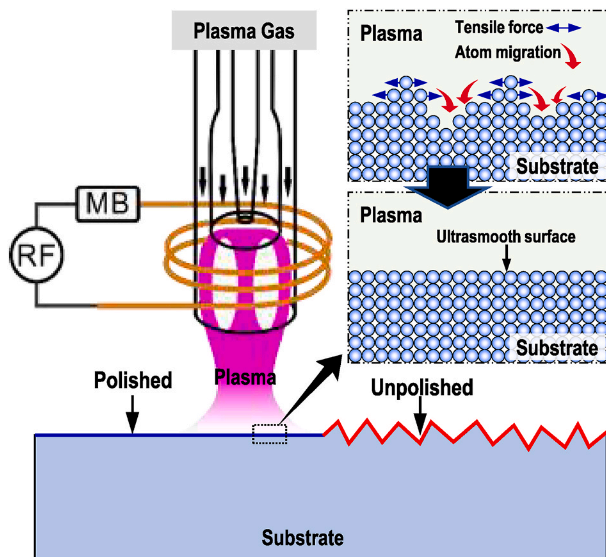

Fig. 1. Schematic diagram of PAMM.

Table 1
Conditions of PAMM of fused silica.

Parameters	Values
Specimen	20 × 20 mm^2, ground surface
Power frequency	40.68 MHz
RF power of plasma	300–1100 W
Gas flow rate	Central gas: 1.0 slm pure Ar Cooling gas: 18 slm pure Ar
Scanning speed	100 mm/min
Scanning pitch	0.5 mm
Quartz tube diameter	18 mm
Gap of plasma jetting	15 mm (tube outlet to substrate)

itself should not react with the work surface without the aid of the catalyst. During processing, the topmost area on the work surface more frequently contacted with the catalyst, and chemical etching proceeded at the contacted areas. Accordingly, the topmost parts of the work surface were preferentially etched and removed and the rms roughness was reduced from 0.173 nm to 0.046 nm. PAP combined the irradiation of atmospheric pressure water vapor plasma and dry CeO_2 abrasive polishing to obtain an atomically flat 4HSiC surface. In this process, a thin SiO_2 layer generated owing to the oxidation of water vapor plasma. It constituted an atomically flat interface between SiO_2 and SiC. Then through the mechanical removal of silicon oxide as well as silicon oxycarbide layers by CeO_2 abrasive, an ultrasmooth surface of 4H–SiC (0001) with rms roughness of 0.1 nm was obtained.

In general, the prior motivation of polishing is to smoothen a surface, it is reasonable to utilize some abrasion-based subtractive approaches to preferentially remove the peak sites. In the existing subtractive polishing processes, smooth surfaces can be eventually obtained by reducing the height difference between peak and valley sites through removing surface material. Since the reduction of the height difference between peak and valley sites plays the key role in polishing, material subtraction is not a necessary condition to achieve an ultrasmooth surface. It is undisputed that a surface is also smoothened when the valley sites are filled by atoms from the peak sites, which can be defined as nonsubtractive surface smoothing technology. As the rapid development of optical industry over the last decades, new manufacturing processes based on high-energy laser beam have been widely developed, in which laser polishing has been investigated by various researches to reduce surface roughness [20,21]. Laser polishing is mainly based on melting caused by thermal input of laser irradiation. While a laser beam of sufficient energy density impinges on material surface, the molten pool can be formed quickly, liquid material tends to rearrange due to surface tension and gravity. When laser beam left, surface temperature of laser irradiated area will drop quickly, leading to molten pool solidified and surface roughness reduced correspondingly [22,23]. In recent years, laser polishing of metallic materials has shown promising results. Marimuthu et al. studied surface polishing of selective laser melting manufactured Ti–6Al–4V components using a continuous wave fiber laser at 1070–1090 nm wavelength and achieved a reduction of surface roughness from 10.2 μm to 2.4 μm [24]. Bordatchev et al. contrasted the polishing effect of continuous wave and pulsed lasers on Ni alloy, and both reduced the surface roughness from 10 μm to 2 μm [25]. Ukar et al. studied the application of laser polishing on DIN 1.2379 tool steel by CO_2 laser and high-power diode laser, both obtaining up to 90% roughness reduction with Ra roughness below 0.5 mm [26].

In this study, plasma-induced atom migration manufacturing (PAMM) at the atomic level is proposed for the first time as a nonsubtractive surface smoothing technology. A case study of PAMM of fused silica substrates is conducted. Plasma diagnostics is carried out to investigate the effects of radical density and the temperature of substrate. The smoothing characteristics of PAMM are investigated. Spherical surface polishing and the ability of surface damage recovery by PAMM are also verified by experiments.

2. Principle of PAMM and experimental method

Fig. 1 shows a schematic of the proposed PAMM. The substrate is mounted on a numerically controlled X–Y motion stage. A radiofrequency (RF) powered inductively coupled plasma (ICP) torch is used as the smoothing tool to realize surface smoothing. Atmospheric pressure ICP is a densely ionized plasma source that has a high gas temperature and a high radical density [27,28]. From interaction with ICP, the surface atoms acquire energy from the plasma via thermal transfer and inelastic collisions from the radicals in plasma. The surface first acquires heat from plasma and the original strong covalent bonds become weak. Then some of these weak bonds are broken owing to the collisions from high energy radicals in plasma. Through this way, some Si–O clusters which are flexible are formed on the surface which means that the surface is melted. Once the top surface is melted, atomic rearrangement driven by surface tensile force takes place. Owing to the nonuniformly distributed tensile force, Si–O clusters around the peak sites are migrated to the valley sites. According to the minimum energy principle [29], the surface eventually becomes ultrasmooth. As shown in Fig. 1, the surface atoms from the peak sites fill the valley sites to form a smooth surface. It is worth noting that ICP possesses some unique properties compared with laser polishing and traditional flame/fire polishing. One is the high density of energetic radicals in ICP. The excited radicals will collide with the surface and weaken the bonds between surface atoms which will further promote the migration of atoms or clusters. The other is high purity of plasma composition. Pure argon (Ar) which is chemically stable was used as the plasma ignition gas without any addition of reactive gases. Thus, the chemical composition of the substrate will not be affected after the PAMM process.

Table 1 shows the experimental conditions of the PAMM of fused silica. The radical components in ICP were measured using an optical spectrometer (Ocean Optics, USB4000) with resolution of 1.4 nm FWHM. Substrate temperature was measured by a thermal camera (FLIR T660) and the accuracy was 0.1 °C. Surface roughness was evaluated by atomic force microscope (AFM, Bruker Dimension edge). Subsurface observation was conducted using a transmission electron microscope (TEM, JEM 3200FS) with spatial resolution of 0.19 nm. The raw data for power spectral density (PSD) analysis were acquired by a scanning white light interferometer (SWLI, Taylor Hobson, CCI) and its vertical resolution was 0.01 nm. The profile and roughness curves were measured by a stylus profilometer (Taylor Hobson, Talysurf i200) with vertical

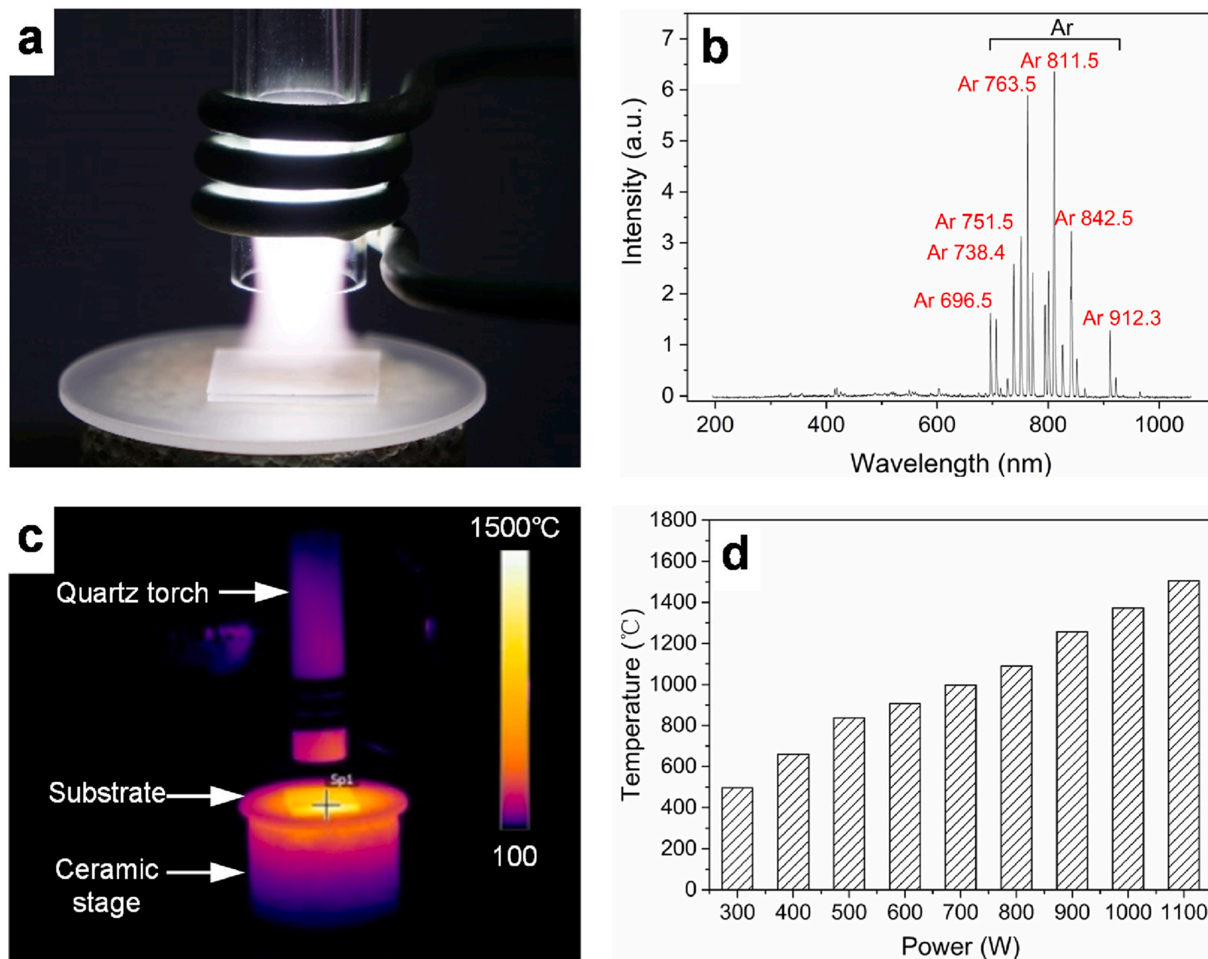

Fig. 2. (a) Photo of the ICP torch. (b) OES spectra of plasma. (c) Infrared thermal image during PAMM. (d) Correlation between substrate surface temperature and applied RF power.

resolution of 16 nm. Scratch damage recovery was confirmed by a confocal laser scanning microscope (CLSM, VK-X250K) with linear scale resolution of 0.5 nm in height measurement.

3. Results and discussion

3.1. Plasma characteristics

According to the mechanism of PAMM, the key factor to realize surface smoothing is the energy transferred by plasma to the substrate surface. Thus, an investigation of the radical components and the substrate temperature under plasma radiation were carried out. Fig. 2a shows a photo of the in-house developed atmospheric pressure ICP torch. Fig. 2b shows the OES spectrum of ICP with an applied power of 600 W. Many peaks corresponding to the emissions from the excited states of Ar atoms were detected. As ICP is considered a highly ionized plasma source [30], it was assumed that a large number of the accelerated Ar^+ ions existed and collided with the fused silica surface.

Fig. 2c shows an infrared thermal image taken during PAMM with an applied power of 1000 W. It is obvious that the area beneath the ICP torch acquired more heat from the plasma and had the highest temperature. Fig. 2d shows the correlation between the average temperature of the substrate area beneath the torch and the applied RF power. When the power was 300 W, the average temperature of the irradiated area was approximately 500 °C. Then, the temperature increased almost linearly with increasing plasma power. With an applied power of 1100 W, the substrate temperature increased to approximately 1500 °C.

It is noteworthy that plasma ignition is an instantaneous process. As the typical thermal conductivity of fused fused silica is 1.3 W/mK, which makes it a large vertical thermal gradient in depth and most of the heat accumulated on the top surface of the specimen. Additionally, the penetration depth of the plasma radicals into the substrate was extremely small; thus, collisions occurred only with the top surface atoms. These two reasons mean the atomic rearrangement happened only on the top surface.

3.2. Smoothing characteristics of PAMM

To investigate the smoothing characteristics of PAMM, the effect of temperature in PAMM, the surface morphology evolution, the changes in surface roughness, subsurface damage and surface waviness distributions were investigated. In PAMM, the surface temperature under the radiation of ICP was the key point to achieve ultrasmooth surface of fused silica, in which the applied RF power was the decisive factor. Thus, the Sa surface roughness variation under different RF power was firstly investigated to explore the highly efficient polishing ability of fused silica. Fig. 3a through d show the surface morphology of fused silica polished by PAMM under different RF power with polishing duration of 6 min. The original surface was processed by diamond grinding. Thus, as shown in Fig. 3a, the surface was rough with a Sa roughness of 86.567 nm. Static treatment by PAMM was carried out on the initially rough surface. When the applied RF power was 600 W, as shown in Fig. 3b, the

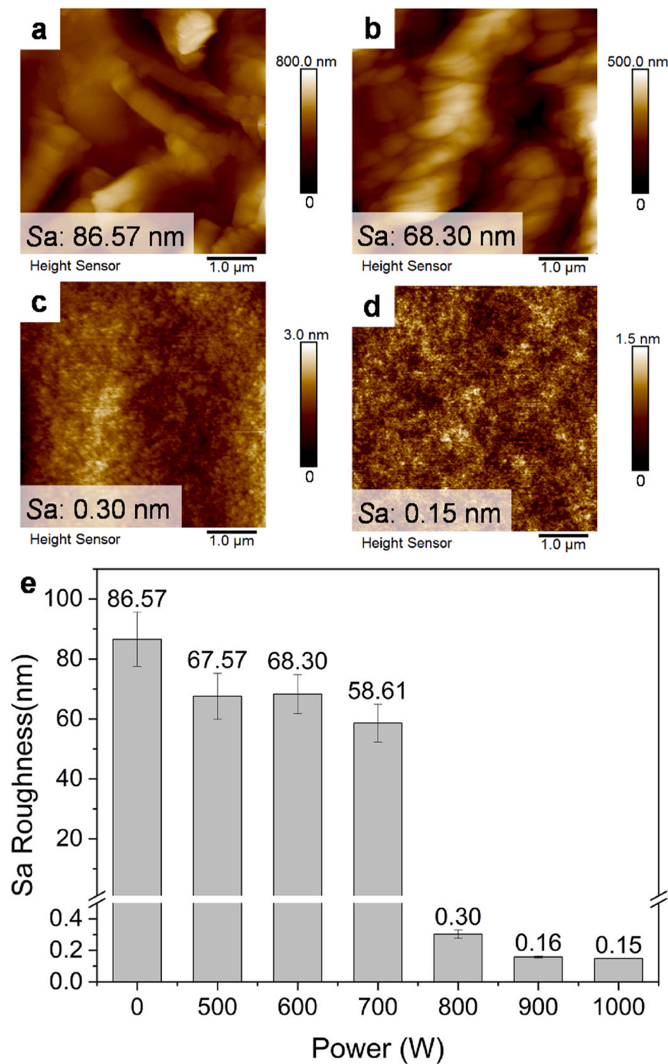

Fig. 3. (a) AFM image of original surface. (b) AFM image of PAMM polished surface under 600 W. (c) AFM image of PAMM polished surface under 800 W. (d) AFM image of PAMM polished surface under 1000 W. (e) Variation of Sa roughness with different RF power.

sharp edges of the micro protrusions on the surface became round and the Sa roughness was slightly decreased. As the RF power increased to 800 W, it can be seen in Fig. 3c that the micro protrusions disappeared and an ultrasmooth surface with Sa roughness of 0.30 nm was obtained. When the RF power reached 1000 W as shown in Fig. 3d, the surface roughness was further decreased to 0.15 nm which demonstrated that an atomic-scale smooth fused silica surface was obtained. Through this it can be seen that high temperature is beneficial to achieve an ultra-smooth surface of fused silica by PAMM.

Fig. 3e shows the detailed surface roughness polished by PAMM with different applied RF powers varying from 500 to 1000 W. While the input RF power was below 800 W, the Sa roughness was slightly decreased owing to the relatively low surface temperature accumulated by ICP radiation. When the applied RF power reached 800 W, the surface polished by PAMM could be dramatically decreased and further reduced to 0.16 nm while RF power increased to 900 W. As it increased to 1000 W, the polished surface maintained an approximately equal Sa roughness value, which represented that the fused silica polished by PAMM might have reached a saturated Sa roughness at 1000 W.

To further demonstrate the saturated Sa roughness of fused silica polished by PAMM, the detailed surface roughness change under 1000 W with prolongation of duration was investigated. As shown in Fig. 4a,

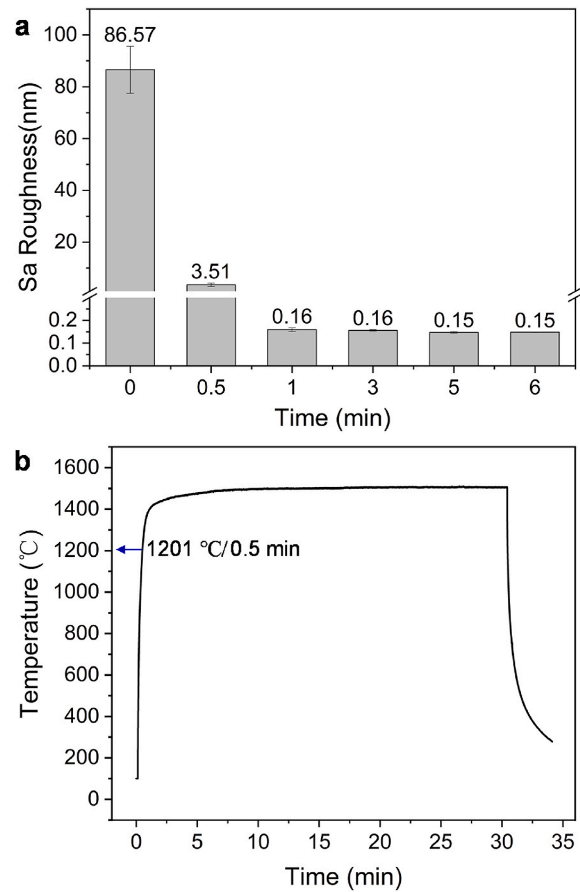

Fig. 4. (a) Variation of *Sa* roughness with different PAMM durations; (b) Temperature curve during PAMM process.

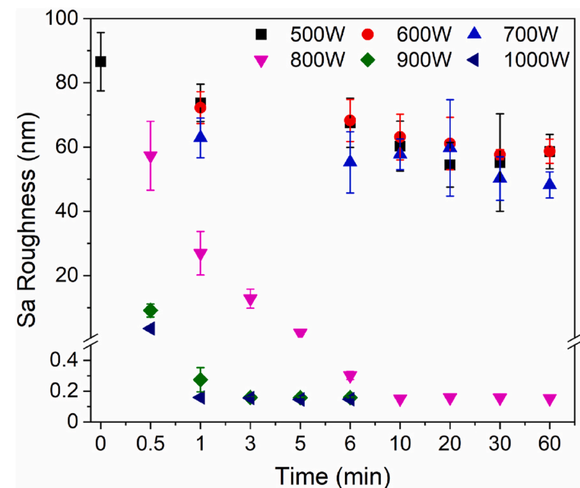

Fig. 5. Variation of Sa roughness with different PAMM durations and RF power.

the *Sa* roughness of fused silica was sharply decreased to 3.51 nm in 0.5 min and reached 0.16 nm as polishing duration increased to 1 min, which represents PAMM is highly efficient for ultraprecision surface smoothing of fused silica. Fig. 4b shows the surface temperature during plasma radiation. It can be found that the surface temperature increased sharply and then became stable for the further increase of duration. After plasma was ignited for 0.5 min, the surface temperature was about 1201 °C which was much lower than the softing point of glass

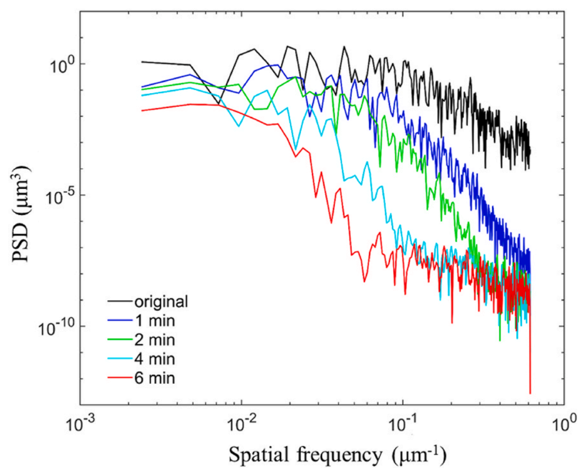

Fig. 6. PSD plot of plasma-polished fused silica surfaces with different durations.

(~1600 °C). Thus, it is considered that temperature was not the only factor determining the smoothing effect of PAMM and the surface dynamics in PAMM process need to be further studied. As the polishing duration further increased, the surface roughness was slightly decreased and became stable at 0.15 nm. According to this, it can be found that fused silica polished by PAMM under 1000 W had reached a saturated Sa roughness of 0.15 nm with polishing duration of 1 min. Conventionally, several steps such as lapping, rough polishing, fine polishing and CMP are required to ultimately achieve an ultrasmooth fused silica surface [31]. In these processes, coolant fluids and polishing slurry are inevitably used. Thus, it can be concluded that PAMM is a highly efficient, low cost and eco-friendly approach for surface smoothing of fused silica.

As the smoothing effect of PAMM is mainly attributed to ICP radiation, there might have different saturated Sa roughness under different RF power as long as the duration is long enough for the surface to reach the equilibrium state of atom/cluster migration of rearrangement. Thus, the variation of Sa roughness with different PAMM durations and RF power was carried out. As shown in Fig. 5, the fused silica polished by PAMM under 1000 W had reached a saturated Sa roughness of 0.15 nm with duration of 1 min. While the RF power was 900 W, it took 3 min to reach a saturated Sa roughness and it was the same value as that of 1000 W. As RF power decreased to 800 W, the Sa roughness was gradually declined and reached the same saturation point with the duration of 10 min. As the further decrease of RF power, the acquired energy was not sufficient and atom migration occurred only at some localized sites, thus, the Sa roughness of fused silica was slightly declined. According to these results, it can be concluded that PAMM can achieve an ultra-smooth surface of fused silica and the ultimate fine surface roughness achieved by PAMM is *S*a 0.15 nm.

The PSD curves of the fused silica surface polished by PAMM were plotted as shown in Fig. 6. The surface morphology data used for calculating the PSD was measured using SWLI with a 410 × 410 μm² area. The surface spatial frequency components (SFCs) with wavelengths of several μm distinctly dropped once the surface was polished for 1 min, but it could not be further reduced by increasing polishing duration. In contrast, the removal of SFCs with wavelengths of several tens of μm became significant as the smoothing duration increased from 1 min to 6 min. However, even when the surface was polished for 6 min, the removal of SFCs with several hundred m wavelength was negligible. These results indicate that atomic rearrangement first occurred locally around the micro peak-valley sites, and then the peak-valleys on the tens μm scale could also be smoothened through atomic migration. However, the smoothing capability over a larger scale was limited because tensile force is only effective in small areas with μm level.

Subsurface quality is an important issue in PAMM as the fused silica surface is completely reconstructed. To verify whether subsurface damages were introduced in PAMM process, cross-sectional observation of the processed surface via TEM was carried out as shown in Fig. 7. A composite protective layer consisting of a layer of carbon and a layer of Pt coated by ion beam deposition was deposited on the surface to avoid the damage introduced by the FIB process during sample preparation. As the deposition of Pt may damage the fused silica surface, a layer of carbon protection had been coated by carbon pen painting. The carbon layer was in liquid form just after being painted by a carbon pen, and it could solidify in a few seconds. Thus, no damage caused by ion bombardment will be introduced in this process. And the Pt protection layer was deposited on the top of the carbon protection layer. As shown in Fig. 7a, there exists some microcracks on the subsurface layer caused by diamond grinding. It is clear that no pores and thermal cracks were formed during PAMM as shown in Fig. 7b and c. Additionally, solidification layer beneath the top surface can't be observed. It is concluded that atomic rearrangement only occurred on the top surface layer with limited atoms involved and the subsurface was not destroyed.

3.3. Scanning polishing by PAMM

To investigate the smoothing characteristics of PAMM of largesize substrates, scanning smoothing on a 20 × 20 mm² fused silica substrate was carried out. Fig. 8a shows the topography of the initial rough substrate. Plasma raster scanning was conducted on both sides of the substrate as shown in Fig. 8b. As a result, a transparent fused silica substrate with mirror surfaces was obtained as shown in Fig. 8c. Before and after

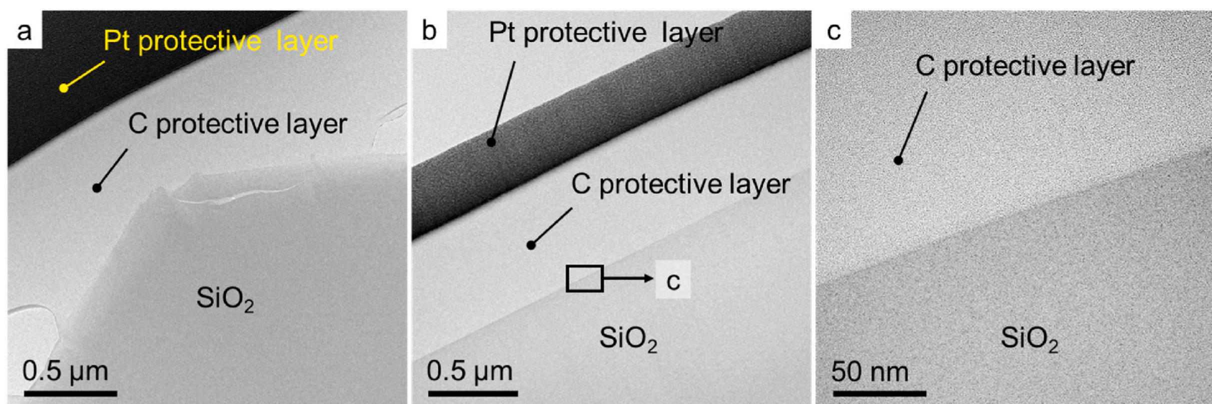

Fig. 7. Subsurface investigation performed by TEM. (a)TEM images of original surface. (b, c) PAMM-polished surface for 6 min.

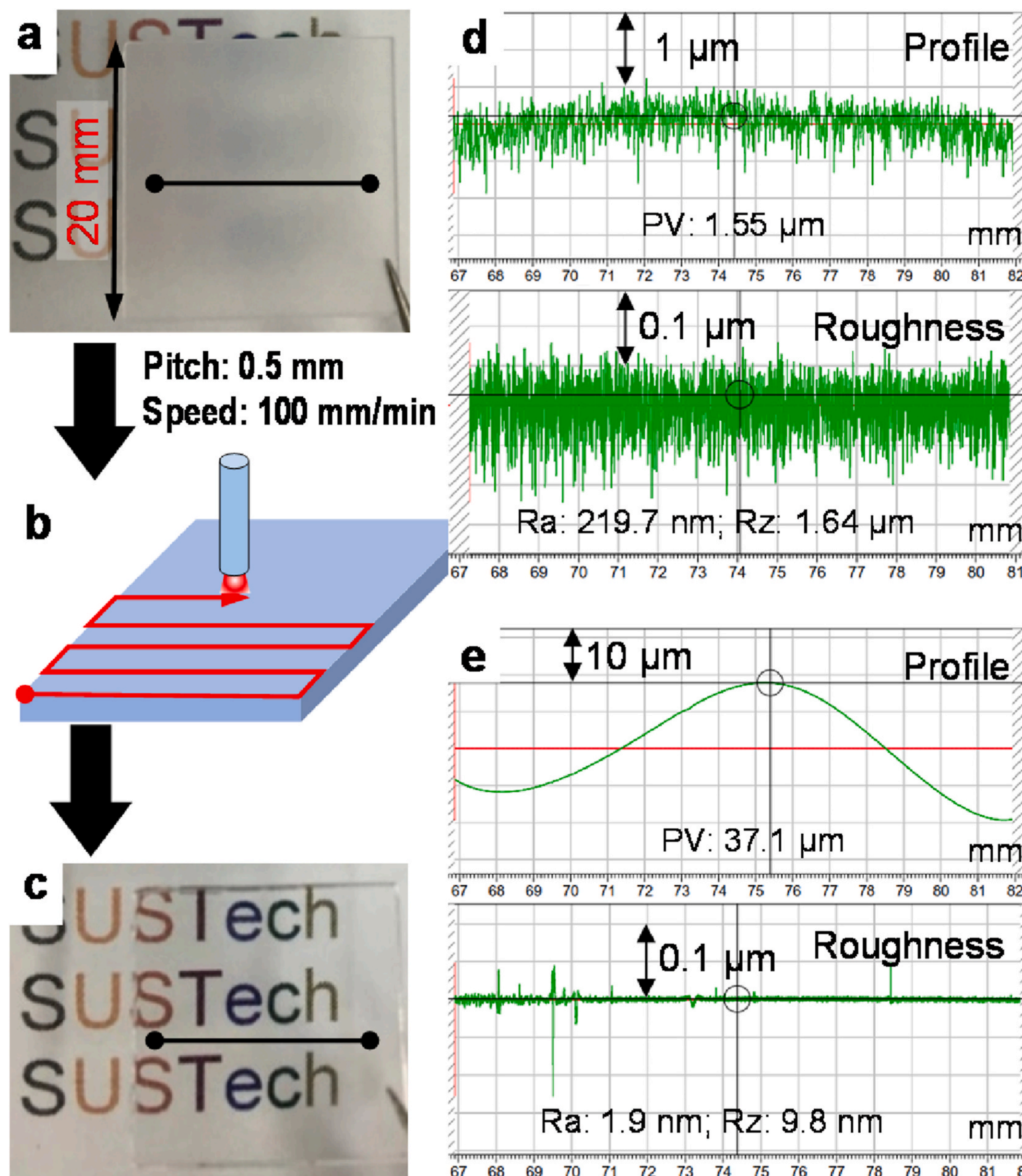

Fig. 8. (a) Photo of the raw substrate. (b) Schematic of plasma scanning polishing. (c) Photo of the polished substrate. (d) Profile and roughness curves of the raw substrate. (e) Profile and roughness curves of the polished substrate.

the smoothing process, the weight of the substrate was measured by a high precision balance. The weight change was negligible indicating that the proposed PAMM process is a nonsubtractive smoothing approach. Fig. 8d and e shows the surface profiles and roughness curves before and after scanning smoothing. Although the substrate was significantly smoothened, form error was introduced. The polishing conditions of PAMM need to be optimized to eliminate this form error.

Besides, the Sa roughness distribution of the entire polished surface was measured to verify the roughness uniformity of PAMM polishing. As shown in Fig. 9, the polished surface was divided into 64 quadrate areas with an interval of 2.5 mm, the represented Sa roughness was the average value tested for three times randomly. It can be found that the whole surface polished by PAMM reaches an atomic level with Sa roughness below 0.2 nm in which the maximum value is 0.188 nm and the minimum value is 0.115 nm. Based on this, it can be concluded that PAMM can achieve an ultrasmooth surface of fused silica with good roughness uniformity, making it a promising technique for large scale optical fused silica components polishing.

3.4. Spherical surface polishing by PAMM

To demonstrate the ability of PAMM in polishing components with curved mirror, experiments were conducted to polish a fused silica component with spherical surface. Fig. 10a shows the image of raw component machined by grinding, the surface was rough and non-transparent. PAMM polishing was conducted on both sides of the substrate, as a result, a transparent fused silica substrate with mirror surfaces was obtained as shown in Fig. 10b. Fig. 10c shows the section profile of original and polished surface tested by stylus profilometer and form error before and after polishing, there was a form error with PV 11.7 μm introduced by PAMM owing to the atoms and clusters rearrangement driven by surface tension and gravity. The roughness change before and after polishing is shown in Fig. 10d, the Ra roughness was decreased from 1.10 μm to 21.3 nm. Based on the results of Fig. 9, PAMM is also effective to polish fused silica components with spherical surface.

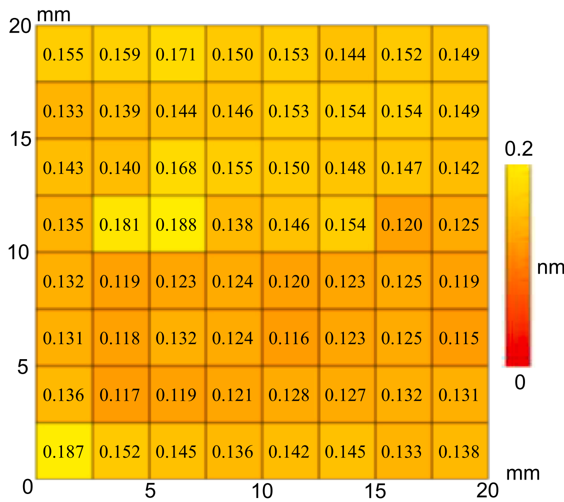

Fig. 9. Sa roughness distribution of fused silica surface polished by PAMM.

3.5. Surface damage recovery by PAMM

Based on the smoothing results, surface rearrangement by ICP-induced atomic fluxion was proven. Since it is possible to move atoms from protruding sites to fill valley sites, the use of PAMM for surface damage recovery is also promising. Fig. 11a shows the morphology and profile of scratches on fused silica formed by a diamond pen. These scratches were several micrometers in depth. Identical site observation by SLCM was carried out and the results are shown in Fig. 11b through d. These scratches were gradually recovered by PAMM. With the prolongation of the duration, the scratch-free areas became ultrasmooth while the scratches became increasingly shallow and eventually disappeared.

These results demonstrate that PAMM is capable of recovering the damaged surface of fused silica. In conventional subtractive smoothing approaches, when a scratch or a crack is formed on the surface, the removal depth of smoothing must be larger than that of the damaged sites to completely remove the sites. Thus, a large volumetric removal, which is not cost and economically efficient, is indispensable. With the application of the proposed PAMM, damage with μm dimensions can be efficiently recovered via a nonsubtractive way.

4. Conclusions and outlook

PAMM was proposed as a nonsubtractive ultra-precision smoothing technology. The ICP torch was characterized by high temperature and high radical density which ensured that the fused silica received sufficient energy to realize surface atomic rearrangement. PAMM was capable of quickly smoothing a ground fused silica surface, with a reduction in Sa roughness from 86.57 nm to below 0.15 nm over an area of 20 × 20 μm^2. In addition, PSD analysis also proved the removal of surface waviness. Surface smoothing of large substrates was successfully conducted by ICP scanning. Finally, PAMM also demonstrated the spherical surface polishing and surface damage recovery capabilities of fused silica.

As PAMM is based on the atomic rearrangement, it would be meaningful to further develop PAMM as general ultra-precision smoothing approach. Additionally, atomic fluxion inevitably changes the surface profile, so it is a great challenge to polish a patterned surface. Future research activities will focus on the application of PAMM on other materials including semiconductors and metals and the applicability of PAMM to polish curved and textured surfaces.

Declaration of competing interest

The authors declare that they have no known competing financial interests or personal relationships that could have appeared to influence the work reported in this paper.

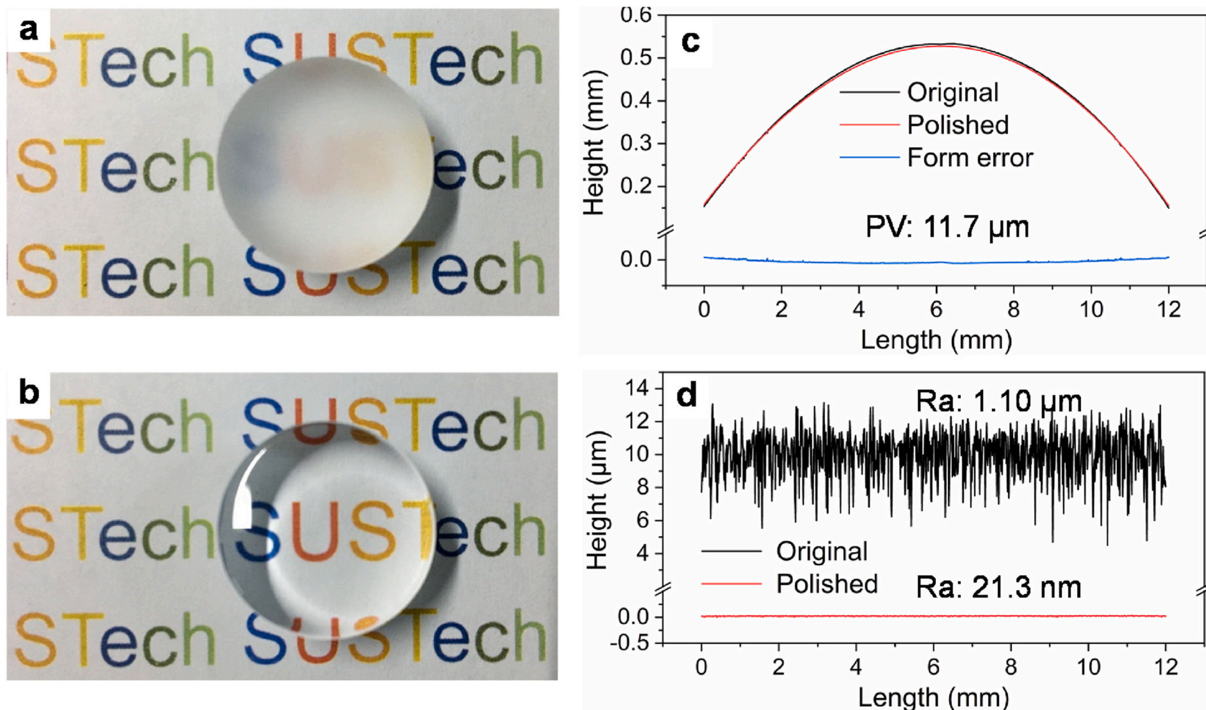

Fig. 10. Spherical surface polished by PAMM. (a) Image of original surface. (b) Image of polished surface. (c) Cross-section profile of original and polished surface. (d) Ra roughness profile of original and polished surface.

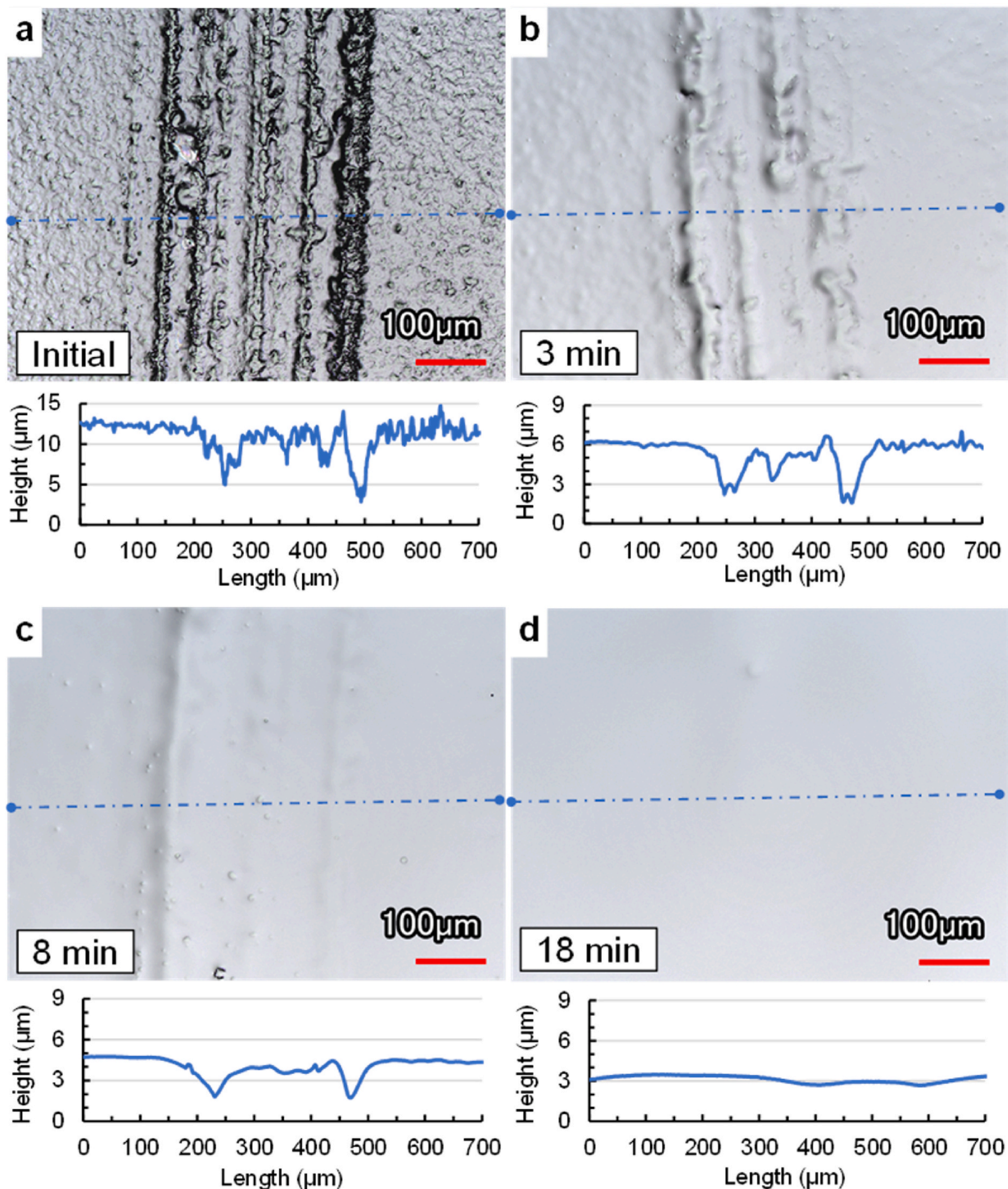

Fig. 11. Variation of morphologies and profiles in scratch recovery by PAMM observed by SLCM.

Acknowledgements

This project is supported by the National Natural Science Foundation of China (52035009, 52005243) and the Science and Technology Innovation Committee of Shenzhen Municipality (JCYJ20200109141003910, JCYJ20210324120402007, KQTD20170810110250357). The authors acknowledge the assistance of SUSTech Core Research Facilities.

References

[1] Hashimoto F, Yamaguchi H, Krajnik P, Wegener K, Chaudhari R, Hoffmeister H-W, Kuster F. Abrasive fine-finishing technology. CIRP Annals 2016;65:597–620.

[2] Lauwers B, Klocke F, Klink A, Tekkaya AE, Neugebauer R, McIntosh D. Hybrid processes in manufacturing. CIRP Annals 2014;63:561–83.

[3] Aida H, Takeda H, Kim S-W, Aota N, Koyama K, Yamazaki T, Doi T. Evaluation of subsurface damage in GaN substrate induced by mechanical polishing with diamond abrasives. Appl Surf Sci 2014;292:531–6.

[4] Zhao D, Lu X. Chemical mechanical polishing: theory and experiment. Friction 2013;1:306–26.

[5] Deng H, Monna K, Tabata T, Endo K, Yamamura K. Optimization of the plasma oxidation and abrasive polishing processes in plasma-assisted polishing for highly effective planarization of 4H-SiC. CIRP Annals 2014;63:529–32.

[6] Aida H, Doi T, Takeda H, Katakura H, Kim S-W, Koyama K, Yamazaki T, Uneda M. Ultraprecision CMP for sapphire, GaN, and SiC for advanced optoelectronics materials. Curr Appl Phys 2012;12:S41–6.

[7] Forsberg M. Effect of process parameters on material removal rate in chemical mechanical polishing of Si(100). Microelectron Eng 2005;77:319–26.

[8] Wang YG, Zhang LC, Biddut A. Chemical effect on the material removal rate in the CMP of silicon wafers. Wear 2011;270:312–6.
[9] Shi X-L, Chen G, Xu L, Kang C, Luo G, Luo H, Zhou Y, Dargusch MS, Pan G. Achieving ultralow surface roughness and high material removal rate in fused silica via a novel acid SiO2 slurry and its chemical-mechanical polishing mechanism. Appl Surf Sci 2020;500.
[10] Wang L, Zhang K, Song Z, Feng S. Ceria concentration effect on chemical mechanical polishing of optical glass. Appl Surf Sci 2007;253:4951–4.
[11] Zhou Y, Pan G, Gong H, Shi X, Zou C. Characterization of sapphire chemical mechanical polishing performances using silica with different sizes and their removal mechanisms. Colloids Surf A Physicochem Eng Asp 2017;513:153–9.
[12] Pan G, Zhou Y, Luo G, Shi X, Zou C, Gong H. Chemical mechanical polishing (CMP) of on-axis Si-face 6H-SiC wafer for obtaining atomically flat defect-free surface. J Mater Sci Mater Electron 2013;24:5040–7.
[13] Shi X, Pan G, Zhou Y, Gu Z, Gong H, Zou C. Characterization of colloidal silica abrasives with different sizes and their chemical–mechanical polishing performance on 4H-SiC (0001). Appl Surf Sci 2014;307:414–27.
[14] Gong H, Pan G, Zhou Y, Shi X, Zou C, Zhang S. Investigation on the surface characterization of Ga-faced GaN after chemical-mechanical polishing. Appl Surf Sci 2015;338:85–91.
[15] Sabia R, Stevens HJ. Performance characterization of cerium oxide abrasives for chemical-mechanical polishing of glass. Mach Sci Technol 2000;4:235–51.
[16] Dong Z, Ou L, Kang R, Hu H, Zhang B, Guo D, Shi K. Photoelectrochemical mechanical polishing method for n-type gallium nitride. CIRP Annals 2019;68: 205–8.
[17] Toh D, Bui PV, Isohashi A, Kidani N, Matsuyama S, Sano Y, Morikawa Y, Yamauchi K. Catalyzed chemical polishing of SiO2 glasses in pure water. Rev Sci Instrum 2019;90:045115.
[18] Deng H, Yamamura K. Atomic-scale flattening mechanism of 4H-SiC (0 0 0 1) in plasma assisted polishing. CIRP Annals 2013;62:575–8.
[19] Fang F, Zhang N, Guo D, Ehmann K, Cheung B, Liu K, Yamamura K. Towards atomic and close-to-atomic scale manufacturing. Int. J. Extreme Manuf. 2019;1.
[20] Guo B, Sun J, Hua Y, Zhan N, Jia J, Chu K. Femtosecond laser micro/nano-manufacturing: theories, measurements, methods, and applications. Nanomanuf. Metrol. 2020;3:26–67.
[21] Kobayashi T, Yan J. Generating nanodot structures on stainless-steel surfaces by cross scanning of a picosecond pulsed laser. Nanomanuf. Metrol. 2020;3:105–11.
[22] Pfefferkorn FE, Duffie NA, Morrow JD, Wang Q. Effect of beam diameter on pulsed laser polishing of S7 tool steel. CIRP Annals 2014;63:237–40.
[23] Wang Q, Morrow JD, Ma C, Duffie NA, Pfefferkorn FE. Surface prediction model for thermocapillary regime pulsed laser micro polishing of metals. J Manuf Process 2015;20:340–8.
[24] Marimuthu S, Triantaphyllou A, Antar M, Wimpenny D, Morton H, Beard M. Laser polishing of selective laser melted components. Int J Mach Tool Manufact 2015;95: 97–104.
[25] Bordatchev EV, Hafiz AMK, Tutunea-Fatan OR. Performance of laser polishing in finishing of metallic surfaces. Int J Adv Manuf Technol 2014;73:35–52.
[26] Ukar E, Lamikiz A, López de Lacalle LN, del Pozo D, Arana JL. Laser polishing of tool steel with CO2 laser and high-power diode laser. Int J Mach Tool Manufact 2010;50:115–25.
[27] Zhang Y, Li R, Zhang Y, Liu D, Deng H. Indiscriminate revelation of dislocations in single crystal SiC by inductively coupled plasma etching. J Eur Ceram Soc 2019;39: 2831–8.
[28] Li R, Zhang Y, Zhang Y, Liu W, Li Y, Deng H. Plasma-based isotropic etching polishing of synthetic quartz. J Manuf Process 2020;60:447–56.
[29] Callen HB, Scott HL. Thermodynamics and an introduction to thermostatistics. Am J Phys 1998;66:164–7. second ed.
[30] Hopwood J. Review of inductively coupled plasmas for plasma processing. Plasma Sources Sci Technol 1992;1:109–16.
[31] Namba Y, Abe M, Kobayashi A. Ultraprecision grinding of optical glasses to produce super-smooth surfaces. CIRP Annals 1993;42:417–20.